IOPscience iopscience.iop.org

Home Search Collections Journals About Contact us My IOPscience

Raman spectroscopy of Si-rich SiO_2 films: possibility of Si cluster formation

This article has been downloaded from IOPscience. Please scroll down to see the full text article.

1996 J. Phys.: Condens. Matter 8 4823

(http://iopscience.iop.org/0953-8984/8/26/014)

View the table of contents for this issue, or go to the journal homepage for more

Download details:
IP Address: 171.66.16.206
The article was downloaded on 13/05/2010 at 18:16

Please note that terms and conditions apply.

J. Phys.: Condens. Matter **8** (1996) 4823–4835. Printed in the UK

Raman spectroscopy of Si-rich SiO_2 films: possibility of Si cluster formation

Y Kanzawa†, S Hayashi‡ and K Yamamoto‡

† Division of Science of Materials, The Graduate School of Science and Technology, Kobe University, Rokkodai, Nada, Kobe 657, Japan

‡ Department of Electrical and Electronics Engineering, Faculty of Engineering, Kobe University, Rokkodai, Nada, Kobe 657, Japan

Received 24 November 1995, in final form 19 March 1996

Abstract. Si-rich SiO_2 films were prepared by a RF cosputtering method and their Raman, infrared absorption and photoluminescence (PL) spectra were measured as functions of Si concentration and annealing temperature. The Raman spectrum was found to change depending on the Si concentration and annealing temperature and differ from those of well known various types of Si. Characteristic features of the spectra are in good qualitative agreement with the theoretical results of a phonon density of states in Si clusters (Si_{33} and Si_{45}) calculated by Feldman *et al*. The present Raman spectra are thus concluded to arise from the Si clusters formed in the films. The spectral changes depending on the excess Si concentration and annealing temperature can be explained in terms of the change in the average size of the clusters. The films also exhibited PL in the visible region. Good correlation between the Raman and PL spectra leads us to conclude that the PL arises from the Si clusters in the films.

1. Introduction

Since Canham's [1] report of strong photoluminescence (PL) in the visible region emitted by anodically oxidized Si, i.e. porous Si, extensive experimental and theoretical studies have been made on the optical properties of nanostructures made of group IV elements. The PL spectra have been reported so far for a wide variety of nanostructures including porous Si, Si nanoparticles [2–4], Ge nanoparticles [5] and C clusters [6]. One of the key issues in these studies is to clarify the quantum size effects caused by the confinement of electrons and holes in zero-dimensional quantum well structures (quantum dots). However, the PL properties of these materials are rather complex, being strongly dependent on the morphology, size and nature of surface layers (passivation by H or O atoms, formation of siloxene derivatives, oxide formation, etc) of the nanostructures. Owing to the complexity of the PL properties, the origin of the PL in the visible region is not yet well understood.

In our previous work [7], we demonstrated that SiO_2 films containing excess Si atoms (Si-rich SiO_2 films), which are prepared by RF cosputtering of Si and SiO_2, exhibit a broad PL peak at almost the same photon energy (about 1.7 eV) as the red-PL peak of porous Si. From various experimental results, including those of infrared (IR) absorption and Raman scattering measurements and transmission electron microscopy (TEM), we suggested that Si structures responsible for the observed PL peak are not Si nanoparticles several nanometres in size, but Si clusters smaller than about 2 nm. Recently, Schuppler *et al* [8] performed x-ray absorption measurements on a series of oxidized Si nanoparticles and a variety of

0953-8984/96/264823+13$19.50 © 1996 IOP Publishing Ltd

porous Si samples and found that the average size of the Si structures responsible for the visible PL is considerably smaller than any size previously reported. They suggested that the visible PL (at about 2 eV) is associated with particles of dimensions typically less than about 1.3 nm, which are well below easy detection with TEM or electron diffraction. In view of our own experimental results and those of Schuppler *et al*, roles played by Si clusters in the visible PL and other optical properties deserve further detailed studies.

Raman spectroscopy is thought to be one of the most effective non-destructive ways of investigating semiconductor clusters. In fact, Honea *et al* [9] have successfully measured Raman spectra of size-selected Si_4, Si_6 and Si_7 clusters by applying a technique of surface-enhanced Raman scattering. They could determine the cluster structures from an analysis of the sharp lines observed. For Ge clusters, although their size was not known and not size selected, Fortner *et al* [10] measured Raman spectra and reported that the spectra resemble that of amorphous Ge but are significantly shifted to lower frequencies. Although these studies demonstrated the applicability of Raman spectroscopy to semiconductor clusters, Raman studies of the semiconductor clusters have been limited so far to only a few cases. Feldman *et al* [11] have calculated the vibrational density of states (DOS) for the magic-number Si clusters Si_{33} and Si_{45}. They found that in a Si_{33} cluster there exist adatom vibrations that are similar in character to modes of the 7×7 reconstructed Si(111) crystalline surface. The frequencies of the adatom vibrations were predicted to be higher than the highest bulk mode in crystalline Si (c-Si) or amorphous Si (a-Si). Experimental observation of such high-frequency split-off modes in relatively large Si clusters has not yet been reported.

In an attempt to confirm the existence of Si clusters in Si-rich SiO_2 films and to explore the Raman spectra of relatively large Si clusters, we have performed systematic Raman studies of Si-rich SiO_2 films. Raman spectra were measured for as-deposited Si-rich SiO_2 films having various concentrations of excess Si atoms as well as for the films annealed in high vacuum. The spectra obtained are to some extent similar to those of a-Si films but considerably different from them in several aspects. One of the remarkable features in our spectra is the appearance of Raman signals around 550 cm^{-1} extending up to 600 cm^{-1}, which are well above the highest phonon frequencies in bulk c-Si or a-Si. The observed overall spectral shapes are in good qualitative agreement with the DOS spectra calculated by Feldman *et al*. The present Raman spectra, therefore, can be attributed to Si clusters formed in Si-rich SiO_2 films. To the present authors' knowledge, this is the first report on the experimental observation of the Raman spectra of Si clusters formed in Si-rich SiO_2 films. We also measured the PL spectra of the samples as a function of the annealing temperature and Si concentration. The peak of the PL spectra exhibited a red shift with increasing annealing temperature or increasing Si concentration. These results confirm our previous suggestion that the visible PL peak located at energies larger than about 1.6 eV is due to Si clusters smaller than about 2 nm and is not due to well grown nanoparticles larger than about 2 nm [7].

2. Experimental procedures

Si-rich SiO_2 films were prepared by a RF cosputtering method similar to that used in our previous work on Ge [12] and Ag [13] microcrystals embedded in SiO_2 matrices. Small pieces of Si wafers 5 mm $\times$ 15 mm $\times$ 0.5 mm in size (Si targets) were placed on a pure SiO_2 target (purity 99.99%; diameter 4 in) and they were cosputtered in Ar gas at 2×10^{-2} Torr with a RF power of 200 W, using an Anelva SPF210HS magnetron sputtering apparatus. The substrates used were Si wafers for IR absorption measurements, either Si wafers or

sapphire plates for Raman measurements, and fused-quartz plates for PL measurements. The substrates were not intentionally heated during the sputtering. Therefore, the substrate temperatures were kept lower than about 100 °C. In this method, the number of excess Si atoms in SiO_2 is roughly proportional to the number of Si targets used. In the present work, the number of Si targets was varied from 0 to 24. Hereafter, the number of Si targets is used to specify the samples and the samples are denoted as Si–N, where N is the number of Si targets. For IR absorption and Raman measurements, in order to keep the total number of excess Si atoms in the films roughly constant, the film thickness was varied from about 0.2 to about 2 μm. Namely, for higher excess Si concentrations, thinner films were deposited. For PL measurements, films about 1 μm thick were deposited to obtain sufficiently high PL intensities. Thermal annealing of the films was performed in a vacuum of 3×10^{-6} Torr for 30 min at various temperatures (200–800 °C). After thermal annealing, the films remained continuous and uniform, i.e. degradation of the films did not occur.

Raman measurements were carried out in a 90° scattering configuration at room temperature. The spectra were recorded with a Spex-Ramalog 5 M spectrophotometer, equipped with a double monochromator and a photon-counting system. The excitation source was the 488.0 nm line of an Ar^+ laser and its power was about 100 mW on the sample. When the Raman spectra are measured in air, Raman signals of air in the low-frequency (less than 200 cm^{-1}) range are usually superimposed on the signals from the sample. In order to eliminate the Raman lines of air, all measurements were carried out by spraying Ar gas on the sample. IR absorption spectra were measured using a Perkin–Elmer 1600 Fourier-transform IR spectrometer. A bare Si substrate was used as a reference. PL spectra were obtained using a Jobin–Yvon U-1000 double monochromator equipped with a photon-counting system. The 325.0 nm line of a He–Cd laser was used to excite the spectra. For the PL spectra, the spectral response of the detection system was corrected with the aid of a reference spectrum of a standard tungsten lamp.

3. Results and discussion

3.1. Infrared absorption spectroscopy

Before presenting the Raman results, we first clarify the characteristics of the present samples by presenting our results of IR absorption measurements. Figure 1 shows the dependence of the IR absorption spectrum on the concentration of excess Si. On the right-hand side of each spectrum, the number of Si targets placed on a SiO_2 target during the sputtering is given. The spectrum of a pure SiO_2 film prepared without Si targets (i.e. the number of Si targets is zero) is also shown. All the spectra were obtained for the as-deposited samples. For comparison, the spectra were normalized at their maximum values and displaced for clarity.

In the frequency range between 700 and 1400 cm^{-1}, the spectrum of the pure SiO_2 film has two peaks. The strong absorption peak centred at 1080 cm^{-1}, which accompanies a high-frequency shoulder, can be attributed to the asymmetric stretching (AS) motion of oxygen atoms in the Si–O–Si units [14, 15]. The weak peak at around 800 cm^{-1} is due to the bending motion of the oxygen atoms [14, 15]. Although the spectra of the Si-rich SiO_2 films basically maintain the two-peak structure similar to that of the pure SiO_2 film, their peak positions and the spectral shapes change depending on the number of Si targets. As the number of Si targets increases from 0 to 24, the following modifications occur. First, the AS mode shifts from 1080 to 1005 cm^{-1} and the oxygen bending mode also shifts to lower frequencies. Secondly, the shoulder of the AS mode gradually disappears and the full

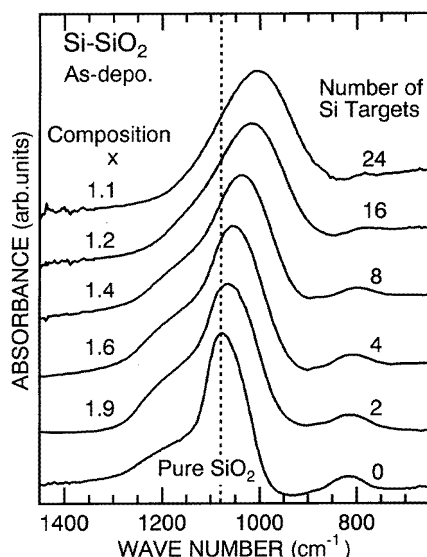

Figure 1. IR absorption spectra of Si-rich SiO_2 films prepared with various numbers of Si targets. The spectrum labelled 0 Si targets was obtained for a pure SiO_2 film. The vertical dotted line indicates the peak position (1080 cm^{-1}) of asymmetric stretching mode of Si–O–Si units in the pure SiO_2 film. All the spectra were normalized at their maximum.

width at half maximum (FWHM) of the AS mode increases. Thirdly, the oxygen bending mode becomes weaker. These behaviours are in fairly good agreement with those previously observed for SiO_x films as x decreases from 2 [16, 17]. If the present samples are regarded as the SiO_x films, from the peak frequency of AS mode, which is known to vary almost linearly with x [14, 16, 17], we can roughly estimate the chemical oxygen concentration x for our samples. The estimated values of x are indicated in figure 1. It is now clear that the Si concentration of the samples increases with increasing number of Si targets.

In figure 2 we show the dependence of the IR absorption spectrum on the annealing temperature T_a for the sample prepared with eight Si targets (sample Si-8). For comparison, the spectrum of the pure SiO_2 films is also shown. For the as-deposited film, the AS mode is very broad and the peak is located at 1036 cm^{-1}. When the film is annealed in high vacuum, with increasing T_a, the AS mode becomes sharper and the shoulder reappears. Simultaneously, the AS mode shifts to higher frequencies and at $T_a = 800\,^{\circ}C$ the peak frequency reaches 1080 cm^{-1}, which is the peak frequency of the pure SiO_2 film.

From previous studies of SiO_x films [18, 19], it is rather well known that, upon annealing in high vacuum, the following reaction takes place in the SiO_x films:

$$2SiO_x \rightarrow xSiO_z + (2-x)Si. \qquad (1)$$

Namely, the decomposition of SiO_x into SiO_2 and elemental Si takes place. After the decomposition, excess Si atoms are expected to form Si clusters embedded in a SiO_2 matrix. The size of the Si clusters is expected to become larger for higher annealing temperatures and higher initial Si concentrations. The changes observed in the IR spectra are consistent with the reaction described by equation (1) and strongly suggest the decomposition of SiO_x and the formation of Si clusters. Unfortunately, the IR spectroscopy does not allow us to obtain direct information on Si clusters. However, as described in detail in the following

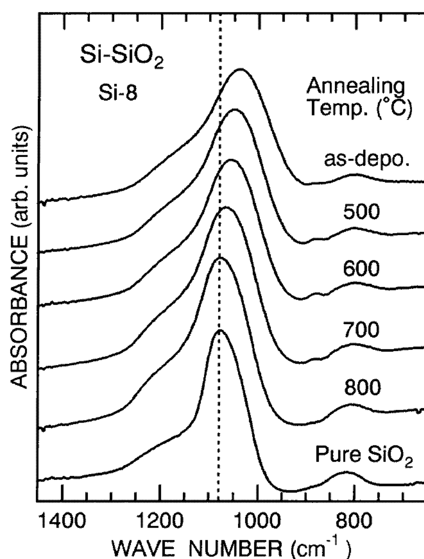

Figure 2. Dependence of IR spectrum on the annealing temperature for sample Si-8. For comparison, an IR absorption spectrum of a pure SiO_2 film is also shown.

section, Raman spectroscopy provides evidence of the formation of Si clusters.

We finally add that H-related absorption peaks (Si–H, $Si–H_2$, etc) similar to those observed for siloxene derivatives [20] did not appear for all the present spectra. Therefore, the siloxene derivatives are not formed in the present samples.

3.2. Raman spectroscopy

3.2.1. Measured spectra. Figure 3 shows Raman spectra of the as-deposited samples with various Si concentrations. A spectrum of a pure SiO_2 film (about 2 μm thick) deposited onto a Si substrate is also shown. These spectra were obtained by subtracting the tails of the PL signals appearing in the high-frequency region of the raw spectra. The figure also includes a Raman spectrum of an a-Si film prepared by sputtering only a Si wafer. The sharp peak at 520 cm^{-1} and weak peak at 300 cm^{-1} (labelled with an asterisk in the figure) are due to the phonon modes of the Si substrate. Since the sample is not strongly absorbent at the excitation wavelength of 488.0 nm, the sharp peak at 520 cm^{-1} is excited by the incident laser beam reaching the substrate. For the samples deposited on the sapphire substrates, the sharp peak at 520 cm^{-1} did not appear and only the broad peaks were observed. Therefore, the Raman signals from the sample layer exhibit no sharp structures.

For the pure SiO_2 film (i.e. the number of Si targets is zero), we cannot see the Raman peaks except for the substrate peaks. However, for the samples containing excess Si atoms, the broad Raman peaks are observed and the spectrum changes depending on the Si concentration. For sample Si-2, although they are not strong, two broad Raman components centred at around 70 and 550 cm^{-1} are clearly seen. Note that the Raman signal around 550 cm^{-1} extends up to 600 cm^{-1}. As the Si concentration increases (samples Si-4 and Si-8), the intensity of the low-frequency component around 70 cm^{-1} increases and a component located around 150 cm^{-1} appears and grows. At the same time, the high-frequency component around 550 cm^{-1} grows and the Raman signals in the intermediate-

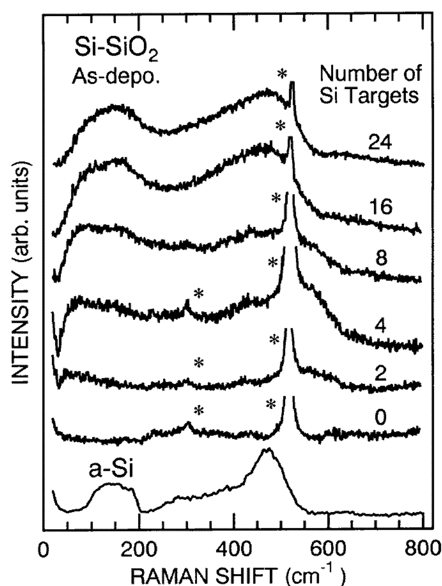

Figure 3. Raman spectra of as-deposited samples prepared with various numbers of Si targets. The spectrum labelled 0 Si targets corresponds to a pure SiO_2 film deposited onto a Si substrate. For comparison, a Raman spectrum of an a-Si film is also shown. The peaks labelled with an asterisk are due to the Si substrate.

frequency (from 200 to 400 cm^{-1}) range appear. As the Si concentration increases further (samples Si-16 and Si-24), the Raman signals extending up to 600 cm^{-1} disappear, a component around 480 cm^{-1} becomes dominant and the low-frequency component around 150 cm^{-1} grows further. It should be noted that, for low Si concentrations (samples Si-2, Si-4 and Si-8), the intensities of the low-frequency components are comparable with that of the high-frequency component. However, as the Si concentration increases (samples Si-16 and Si-24), the high-frequency component around 480 cm^{-1} becomes stronger than the low-frequency component around 150 cm^{-1}.

The annealing-temperature dependence of the Raman spectrum for sample Si-8 is shown in figure 4 together with the spectrum of an a-Si film. The sharp peak at 520 cm^{-1} and the weak peak at 300 cm^{-1} (labelled with an asterisk in the figure) are again due to the Si substrate. In order to prove that these peaks really come from the Si substrate even after annealing the sample, sample Si-8 deposited on a sapphire substrate was annealed at 800 °C. The spectrum obtained after annealing is shown in figure 5. We can see that the sample deposited on the sapphire substrate no longer exhibits the sharp peak at 520 cm^{-1} and the weak peak at around 300 cm^{-1} but exhibits several sharp peaks (labelled with a #) owing to the sapphire substrate. The same results were obtained for the samples annealed at other temperatures. It is now very clear that the present sample exhibits no sharp Raman lines even after annealing.

In figure 4 we see that the spectrum remains almost unchanged upon annealing at 400 °C. However, as the annealing temperature is increased further, the low-frequency component around 150 cm^{-1} grows and the splitting of the low-frequency component becomes apparent. The intensity of the high-frequency shoulder seen at around 550 cm^{-1} first increases, then decreases and finally disappears at $T_a = 800\,^{\circ}C$. For low annealing temperatures

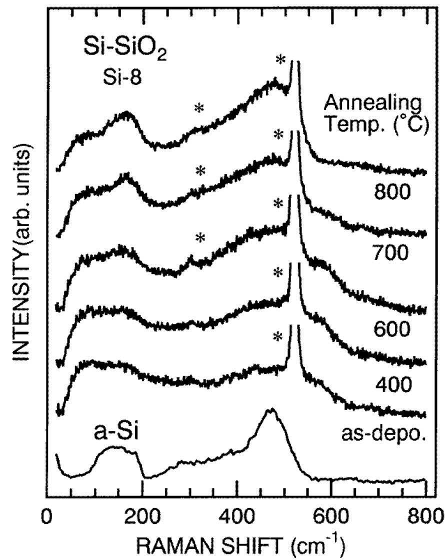

Figure 4. Dependence of Raman spectrum on the annealing temperature for sample Si-8. For comparison, a Raman spectrum of an a-Si film is also shown. The peaks labelled with an asterisk are due to the Si substrate.

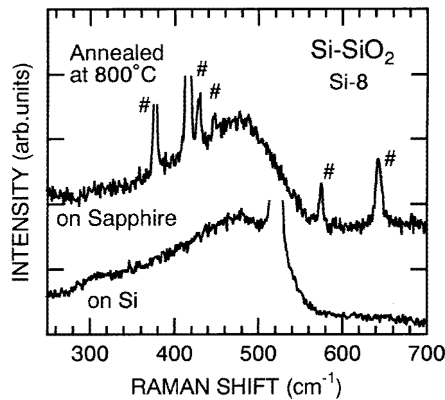

Figure 5. Raman spectra of Si-8 samples annealed at $T_a = 800\,^{\circ}C$ deposited onto a Si substrate and a sapphire substrate. The sharp peaks marked with a # are due to the sapphire substrate.

$T_a = 400$ and $600\,^{\circ}C$, the intensities of the low-frequency components are comparable with that of the high-frequency component but, for higher annealing temperatures, the high-frequency component around 480 cm^{-1} increases and becomes stronger than the low-frequency components. Comparing figure 4 with figure 3 we can note that the spectral changes caused by annealing are very similar to those caused by the increase in the excess Si concentration, although the splitting of the low-frequency component is less pronounced in the concentration dependence shown in figure 3.

It should be noted here that the Raman signals observed for the present samples are not due to the vibrational modes of Si–O–Si bonds in SiO_2. It is well known that the Raman

spectrum of amorphous SiO_2 (a-SiO_2) exhibits a broad feature extending from about 50 to 600 cm^{-1} with a pronounced peak around 420 cm^{-1} [21]. However, the Raman efficiency of a-SiO_2 is not so large and consequently, in the case of thin films, the films should be sufficiently thick (thicker than several micrometres) to give rise to detectable Raman signals. In fact, for our sputter-deposited pure SiO_2 film about 2 μm in thickness (sample Si–0 in figure 3), the Raman signals attributable to the SiO_2 film were hardly detected. Since the Raman spectrum at present observed changes depending on the concentration of excess Si atoms and the annealing temperature, the present Raman signals are thought to come from Si–Si vibrations introduced by excess Si atoms.

Although the present spectra, in particular those of the as-deposited sample Si-24 and sample Si-8 annealed at 800 °C, somewhat resemble that of a-Si, a close comparison reveals that the present spectra considerably differ from that of a-Si. As described above, almost all spectra of as-deposited and annealed samples exhibit a high-frequency shoulder around 550 cm^{-1} extending up to 600 cm^{-1}, while the spectrum of a-Si shows a relatively sharp cut-off around 500 cm^{-1}. Furthermore, the low-frequency component located around 70 cm^{-1} is not present in the spectrum of a-Si. The intensity of the low-frequency component relative to that of the high-frequency component in the present spectra is larger than that of a-Si.

From previous studies [19, 22, 23], it is known that Si microcrystals several nanometres in size can be grown in the Si-rich SiO_2 films by annealing the films at high temperatures. If the present samples contain Si microcrystals several nanometres in size, they would exhibit a sharp Raman peak around 520 cm^{-1} similar to those reported in our previous paper [7]. Since such a sharp peak was not observed for the present samples (as confirmed by the results shown in figure 5), we can rule out the existence of Si microcrystals. The cross-sectional TEM observation of the present samples did not show lattice fringes corresponding to the Si microcrystals, thus confirming the Raman results. The absence of well grown Si microcrystals in our present samples is due to lower initial concentrations of excess Si atoms and lower annealing temperatures than in the previous studies. To our knowledge, spectra similar to those shown in figures 3 and 4 have not been reported so far for c-Si, a-Si, nanostructures of Si and SiO_x films. However, it should be noted that Raman spectra reported by Denisov *et al* [24] for Si–SiO_2 superlattices show features very similar to those observed in this work. The comparison between their and our data will be discussed later.

3.2.2. Interpretation of spectra. We now discuss the origin of the Raman spectra observed. Recently, Feldman *et al* [11] reported the vibrational DOS of Si clusters theoretically, which are in qualitative agreement with the spectral features at present observed. They calculated the DOS spectra for the magic-number clusters Si_{33} and Si_{45}, whose geometric structures were constructed on the basis of the reconstructed structure of the Si surface. The structure of Si_{33} was constructed on the basis of the Si(111) 7×7 surface, and that of Si_{45} on the basis of the Si(111) 2×1 surface. Figure 6 compares the calculated DOS spectra with our typical Raman spectra of samples Si-8 annealed at 400 and 800 °C. In the figure the calculated DOS spectrum and the Raman spectrum of a-Si are also included. Because of the potential used, calculated frequencies of the vibrational modes are somewhat higher than the values which will be measured experimentally. To facilitate the comparison between theory and experiment, the frequency scale of the calculated DOS spectra was so adjusted that the calculated DOS spectrum of a-Si agrees well with the experimental Raman spectrum. Namely, the original frequency scale was reduced by a factor of 0.88 to reduce the high-frequency DOS peak of a-Si to the experimental value of 480 cm^{-1}.

In figure 6 we can see that characteristic features of the experimental spectrum of

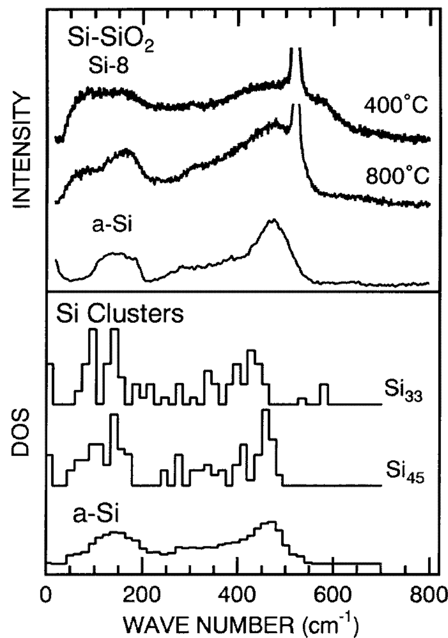

Figure 6. Comparison of the DOS spectra of the Si_{33} and Si_{45} clusters (from [11]) with Raman spectra of sample Si-8 annealed at $T_a = 400$ and $800\,^{\circ}C$.

$T_a = 400\,^{\circ}C$ agree very well with those of the calculated DOS spectrum of Si_{33}. A striking feature in the DOS spectra of Si_{33} is the appearance of high-frequency split-off modes (at 540 and 585 cm^{-1} after rescaling), which are located at higher frequencies than the highest bulk mode for c-Si and a-Si. These split-off modes correspond to adatom vibrations similar to those in the Si(111) 7×7 surface. Furthermore, the calculated DOS spectrum shows a low-frequency component around 70 cm^{-1} in addition to a component around 150 cm^{-1}. The component at 70 cm^{-1} does not appear in the DOS spectrum of a-Si. In the experimental spectrum of $T_a = 400\,^{\circ}C$, Raman signals attributable to these components are seen, although the splitting of the components is not so clear as in the DOS spectrum. In the DOS spectrum, the components around 70 and 150 cm^{-1} are stronger than the high-frequency components around 450 cm^{-1}, in good qualitative agreement with the experimental spectrum.

In the DOS spectrum of the Si_{45} cluster, the high-frequency split-off modes do not appear. The low-frequency component around 70 cm^{-1} becomes weaker than the component around 150 cm^{-1}. Furthermore, the high-frequency component around 480 cm^{-1} becomes stronger than the low-frequency components. These changes in the DOS spectrum agree fairly well with those in the Raman spectrum observed by raising T_a from 400 to $800\,^{\circ}C$. Since the Raman spectrum is determined by not only the DOS but also the matrix elements, the argument based on only the DOS spectrum is not sufficient. Moreover, the calculations of Feldman *et al* were limited to only Si_{33} and Si_{45} clusters. However, from the good qualitative agreement between theory and experiment, we conclude that the present Raman spectra originate from the Si clusters formed in the films. The changes in the spectral shape can be explained in terms of the increase in the size of the Si cluster. In fact, the increase in the average size upon annealing is strongly suggested by the IR results together with the reaction described by equation (1). In as-deposited samples, the Raman results indicate that

the partial clustering of Si atoms already occurred during the deposition. It is very natural to assume that the size of the clusters is determined by the initial Si concentration, i.e. the higher the initial Si concentration, the larger the size of the Si clusters.

The spectra observed at present are rather broad and the split-off modes are not well separated from the rest of the spectra. This may be due to the size distribution of the clusters. The appearance of the split-off modes and the strong low-frequency component in the spectra may not directly indicate the dominance of the Si_{33} cluster in our samples. Although a theoretical analysis is still lacking at present for Si clusters other than Si_{33} and Si_{45}, cluster structures analogous to the Si(111) 7×7 surface and corresponding adatom vibrations may be possible in Si clusters of various sizes. What was observed at present as a high-frequency shoulder may be the Raman signals from various adatom vibrations, with frequencies slightly different from each other, in clusters of various sizes within a size distribution. However, as mentioned above, the average size of the cluster is thought to be increased with increasing excess Si concentration and annealing temperature. Further theoretical calculations of DOS spectra for Si clusters of various sizes are urgently required to analyse in more detail the present experimental spectra.

Fortner *et al* [10] have reported Raman spectra attributable to Ge clusters about 1 nm in diameter. They prepared the Ge clusters by depositing Ge onto carbon films at a coverage less than one monolayer. Their Raman spectra are similar in shape to that of a-Ge. However, they found that spectra are shifted to lower frequencies than that of a-Ge. Furthermore, they found that the intensity ratio of the low-frequency peak to the high-frequency peak is higher than that of a-Ge. Although they did not observed the high-frequency modes located outside the frequency region of bulk phonons in c-Ge and a-Ge, spectral features reported by them agree fairly well with those reported in this paper. The similarity of the observed features supports our assignment of the Raman spectra to the Si clusters.

As mentioned above, Denisov *et al* [24] reported Raman spectra of Si–SiO_2 superlattices made by alternating extremely thin Si layers (thickness equivalent to two or four monolayers) and relatively thick SiO_2 layers. In these samples, they observed spectra very similar to those presented in figures 3 and 4. The intensity ratio of the low-frequency (50–200 cm^{-1}) peak to the high-frequency (350–550 cm^{-1}) peak was found to be higher than that of a-Si. Furthermore, a high-frequency shoulder around 550 cm^{-1} was also observed. As the origin of the larger intensity ratio, Denisov *et al* suggested the localization of the TO phonon mode in a-Si. They assigned the high-frequency shoulder to the interface mode between Si and SiO_2 layers. However, their explanations of the Raman spectra are less appealing, because it is not clear whether or not the interpretation based on bulk a-Si can be applied to very thin Si layers of two or four monolayers. They did not pay much attention to the possibility of the Si cluster formation. Judging from the similarity of their Raman spectra with our own spectra, we suggest that their Raman spectra originate from the aggregated Si atoms, i.e. Si clusters, embedded in SiO_2 matrices.

3.3. Photoluminescence spectroscopy

In our previous paper [7], we reported only the T_a dependence of PL spectra for sample Si-8. We present here the dependence of the PL spectrum on the Si concentration as well as on the annealing temperature and compare them with the Raman spectra observed. The samples for the present PL measurements were newly prepared on fused-quartz plates, because the sapphire plates used in the previous work showed strong PL peaks at about 1.8 eV which complicate the spectra. The excitation source (the 325.0 nm line of a He–Cd laser) and detection system (a Jobin–Yvon U-1000 double monochromator and a photomultiplier) were

also different from those previously used.

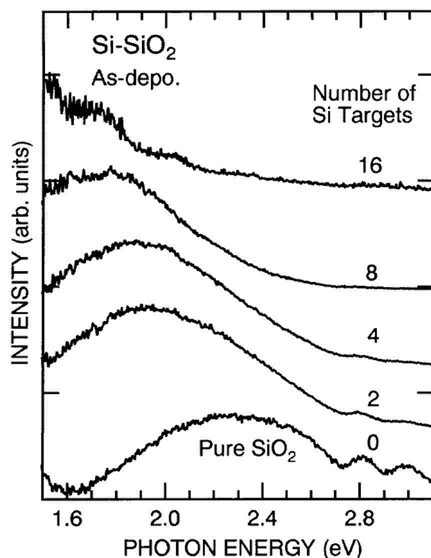

Figure 7. PL spectra of as-deposited samples prepared with various numbers of Si targets. A spectrum of the pure SiO_2 film is also shown.

Figure 7 shows PL spectra of as-deposited samples. For comparison, each spectrum was normalized at the maximum intensities and displaced. The pure SiO_2 film containing no excess Si atoms exhibits a broad PL peak around 2.3 eV. In this energy region, luminescence bands due to various types of defect in a-SiO_2 glasses are well known [25, 26]. Moreover, as has been reported by Hayashi *et al* [6], carbon-doped SiO_2 films show a strong PL peak in the energy range from 2 to 2.4 eV. Therefore, the PL peak at around 2.3 eV may arise from the structural defects in the SiO_2 film and/or the carbon impurities captured by the film during the sputter deposition. For the samples containing excess Si atoms, the broad PL peaks are located at energies below 2 eV. As the number of Si targets increases from two to eight, the peak shifts from 1.9 to 1.6 eV. For sample Si-16, the peak seems to be located outside the spectral region at present explored and only its tail is observed. No detectable PL signals were obtained for sample Si-24 under the present experimental conditions.

The dependence of the PL spectrum on the annealing temperature for sample Si-8 is shown in figure 8. All the spectra are normalized at their maximum intensities and displaced for clarity. For $T_a \leqslant 400\,^{\circ}$C, the spectra are almost unchanged and the peak position is located at about 1.8 eV. However, for $T_a \geqslant 600\,^{\circ}$C, the peak gradually shifts to lower energies as T_a is raised. For $T_a = 800\,^{\circ}$C, the peak reaches 1.55 eV. These spectral changes depending on T_a agree fairly well with our previous data [7].

From a close comparison of the Raman spectra (figure 4) with PL spectra (figure 8) for Si-8 samples, we find good correlation between them. For $T_a \leqslant 400\,^{\circ}$C, both the PL and the Raman spectra remain almost unchanged. On the other hand, for $T_a \geqslant 600\,^{\circ}$C, the PL peak shifts to lower energies and simultaneously the shape of the Raman spectrum changes considerably depending on T_a. For as-deposited samples, the PL spectrum (figure 7) clearly shows the red shift with increasing Si concentration, while the Raman spectrum (figure 3) drastically changes as the Si concentration increases.

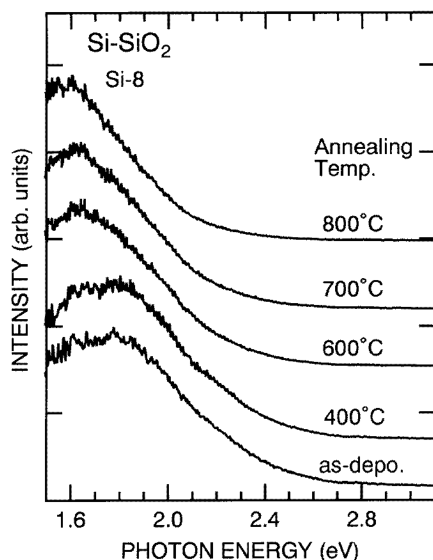

Figure 8. Dependence of the PL spectrum on the annealing temperature for sample Si-8.

As mentioned previously, we can rule out the siloxene derivatives as the origin of the PL peak obtained. In our previous paper [7], we suggested that the PL of Si-rich SiO_2 films arises from the electronic transition between the HOMO–LUMO gap in Si clusters formed in the film. The present good correlation between the PL and Raman spectra confirms this suggestion. The red shift of the PL peak with increasing T_a or Si concentration is explained by the increase in the average size of the clusters. This interpretation is in good qualitative agreement with the theoretical study [27], in which the HOMO–LUMO gap of the Si clusters decreases with increasing size. Although many workers claimed that Si nanocrystals give rise to visible PL, our present and previous data indicate that the Si clusters are very important sources of the PL in the visible region (energy range higher than about 1.6 eV).

4. Conclusion

We have prepared Si-rich SiO_2 films by RF cosputtering of Si and SiO_2 and measured their IR absorption and Raman spectra as functions of Si concentration and annealing temperature. The changes in the IR spectra observed upon annealing the films suggest that the reaction $2SiO_x \rightarrow xSiO_2+(2-x)Si$ proceeds in the films and, consequently, the SiO_x films gradually decompose into SiO_2 regions and aggregates of Si atoms.

The Raman spectra of the films were found to depend on the Si concentration and annealing temperature and differ from those of the previously reported various types of Si, such as microcrystalline Si, bulk c-Si and a-Si. The spectral shapes are in good qualitative agreement with those of the DOS spectra of Si clusters (Si_{33} and Si_{45}) calculated by Feldman *et al* [11]. We can thus attribute the present Raman signals to Si clusters formed in the films. The spectral changes observed on increasing the excess Si concentration and the annealing temperature are explained in terms of the increase in the size of the clusters.

The present samples exhibited a broad PL peak in the visible region (1.6–1.9 eV). A

red shift in the PL peak was observed with increasing annealing temperature and increasing Si concentration. From the good correlation between the Raman and PL spectra, we can conclude that the PL arises from the Si clusters formed in the films.

Although the present results give strong evidence for the formation of Si clusters in the as-deposited and annealed Si-rich SiO_2 films, the size and structure of the clusters are still unknown. Further experimental and theoretical studies are required to gain more insight into the Si clusters formed. The atomic structure of the as-deposited Si-rich SiO_2 films also deserves further studies in connection with the structure of SiO_x films prepared by various methods.

Acknowledgments

This work was supported by a Grant-in-Aid for Scientific Research from the Ministry of Education, Science and Culture, Japan.

References

[1] Canham L T 1990 *Appl. Phys. Lett.* **57** 1046
[2] Takagi H, Ogawa H, Yamazaki Y, Ishizaki A and Nakagiri T 1990 *Appl. Phys. Lett.* **56** 2379
[3] Morisaki H, Ping F W, Ono H and Yazawa K 1991 *J. Appl. Phys.* **70** 1869
[4] Littau K A, Szajowski P J, Muller A J, Kortan A R and Brus L E 1993 *J. Phys. Chem.* **97** 1224
[5] Maeda Y, Tsukamoto N, Yazawa Y, Kanemitsu Y and Masumoto Y 1991 *Appl. Phys. Lett.* **59** 3168
[6] Hayashi S, Kataoka M and Yamamoto K 1993 *Japan. J. Appl. Phys.* **32** L274
[7] Hayashi S, Nagareda T, Kanzawa Y and Yamamoto K 1993 *Japan. J. Appl. Phys.* **32** 3840
[8] Schuppler S, Friedman S L, Marcus M A, Adler D L, Xie Y-H, Ross F M, Harris T D, Brown W L, Chabal Y J, Brus L E and Citrin P H 1994 *Phys. Rev. Lett.* **72** 2648
[9] Honea E C, Ogura A, Murray C A, Raghavachari K, Sprenger W O, Jarrold M F and Brown W L 1993 *Nature* **366** 42
[10] Fortner J, Yu R Q and Lannin J S 1990 *J. Vac. Sci. Technol.* A **8** 3493
[11] Feldman J L, Kaxiras E and Li X-P 1991 *Phys. Rev.* B **44** 8334
[12] Fujii M, Hayashi S and Yamamoto K 1991 *Japan. J. Appl. Phys.* **30** 687
[13] Fujii M, Nagareda T, Hayashi S and Yamamoto K 1991 *Phys. Rev.* B **44** 6243
[14] Pai P G, Chao S S, Takagi Y and Lucovsky G 1986 *J. Vac. Sci. Technol.* A **4** 689
[15] Kirk C T 1988 *Phys. Rev.* B **38** 1255
[16] Schumann L, Lehmann A, Sobotta H, Riede V, Teschner U and Hubner K 1982 *Phys. Status Solidi* b **110** K69
[17] Nakamura M, Mochizuki Y, Usami K, Itoh Y and Nozaki T 1984 *Solid State Commun.* **50** 1079
[18] Rochet F, Dufour G, Roulet H, Pelloie B, Perriere J, Fogarassy E, Slaoui A and Froment M 1988 *Phys. Rev.* B **37** 6468
[19] Nesbit L A 1985 *Appl. Phys. Lett.* **46** 38
[20] Fuchs H D, Stutzmann M, Brandt M S, Rosenbauer M, Weber J, Breitschwerdt A, Deak P and Cardona M 1993 *Phys. Rev.* B **48** 8172
[21] Alben R, Weaire D, Smith J E Jr and Brodsky M H 1975 *Phys. Rev.* B **11** 2271
[22] Hartstein A, Tsang J C, DiMaria D J and Dong D W 1980 *Appl. Phys. Lett.* **36** 836
[23] Olego D J and Baumgart H 1988 *J. Appl. Phys.* **63** 2669
[24] Denisov V N, Mavrin B N, Pudonin F A and Vinogradov E A 1990 *Sov. Phys. Solid State* **32** 1266
[25] Itoh C, Suzuki T and Itoh N 1990 *Phys. Rev.* B **41** 3794
[26] Kuzuu N, Komatsu Y and Murahara M 1992 *Phys. Rev.* B **45** 2050
[27] Ren S Y and Dow J D 1992 *Phys. Rev.* B **45** 6492